Desalination and Water Treatment
www.deswater.com
doi: 10.1080/19443994.2014.895780

54 (2015) 1809–1818
May

Taylor & Francis
Taylor & Francis Group

Thermal analysis of heat transfer performance in a horizontal tube bundle

Shengqiang Shen*, Hua Liu, Luyuan Gong, Yong Yang, Rui Liu

Key Laboratory of Liaoning Province for Desalination, School of Energy and Power Engineering, Dalian University of Technology, 209 Room, Comprehensive Experimental 2 Building, No. 2 Linggong Road, Ganjingzi District, Dalian 116024, Liaoning, China, Tel. +86 411 84708464; Fax +86 411 84707963; email: zzbshen@dlut.edu.cn

Received 23 September 2013; Accepted 31 January 2014

ABSTRACT

The thermal analysis is demonstrated for the case where steam is condensing inside a horizontal tube bundle, while simultaneously thin water films are evaporating outside the tubes generating vapor that flows across the tubes. Three experiments are carried out each coming up with a valid model to predict the impact of the corresponding parameters on the heat transfer performance or flow characteristics. Then, a collective two-dimensional model is established according to the models from those experiments to simulate the thermal and hydrodynamic performance of the evaporator. This model consists of three parts corresponding to the three models obtained from the experiments mentioned above: the water film evaporation model, the inside-tube steam model, and the intertube vapor model. The operating conditions include the water mass rate, saturation temperatures, and overall temperature difference. Calculations are carried out for water mass rate between 0.03 and 0.09 kg/m s, inlet steam temperature between 53 and 73°C, and overall temperature difference between 1.5 and 4°C. Results of the analysis show that the overall heat transfer coefficient and vapor temperatures have uneven distributions within the tube bundle. The variation of vapor temperature affects the distribution of heat transfer rate and the steam inlet velocity. The utilizations of the initial temperature difference with the change of tube bundle column numbers are also analyzed. It shows that the more column numbers the tube bundle includes, the more heat transfer area will lose a certain amount of initial temperature difference.

Keywords: Falling film evaporation; Horizontal tube bundle; Modeling simulation; Flow and heat transfer

1. Introduction

The world is now facing more challenges from the water shortage problem. Rapid development of low-temperature multi-effect distillation (MED) system during recent years provides a promising technology for supplying large quantity of fresh water. The horizontal tube bundle evaporator showing distinct advantages of high heat transfer coefficient, maximum use of available temperature difference, positive venting, good vapor separation, etc. over other evaporators such as the forced circulation, rising film, and falling film vertical tube evaporators, has extensive application in large-scale desalination plants.

In general, the falling film evaporation process for desalination features the brine films flowing downward and evaporating outside the tube bundle surfaces absorbing heat from the inside of the tubes where steam flows and condenses. Numerous theoretical and

*Corresponding author.

experimental studies have been carried out to investigate the effects of various parameters on falling film evaporation heat transfer performance outside a single tube or condensation heat transfer inside circular tubes.

For evaporation outside the horizontal tube, parameters such as the liquid film Reynolds number, evaporation temperature, liquid properties, tube space, and heat flux have been studied as the major parameters that affect the flow and heat transfer performance outside a single horizontal tube or a tube bundle. For convective dominated conditions, according to Fujita et al. [1] and Liu et al. [2], as the Reynolds numbers of the liquid increases, the heat transfer coefficient decreases first, then increases after a minimum value while some others [3,4] report the heat transfer coefficient increases with the Reynolds number. Shen et al. [5] recently proposed a critical value Reynolds number of 450 for seawater below which the heat transfer coefficient increases with the Reynolds number but decreases afterwards. These discrepancies might be attributed to different falling film modes or working fluids. Falling film evaporation on tube bundle exhibits more complexities because of intertube evaporation and liquid splash. Zeng et al. [6] observed an insignificant effect of film Reynolds number and independent of saturation temperature on global heat transfer coefficient for triangular pitch bundle. Xu et al. [7] investigated falling film evaporation performance on a horizontal tube bundle and discussed mutual interactions between shell-side parameters and tube-side parameters. Zeng et al. [8] found in the tube bundle with all the tube surfaces wetted, upper tubes has higher heat transfer coefficients.

For condensation inside circular tubes, numerous flow pattern maps have been proposed over the years for predicting two-phase flow regime transitions in horizontal tubes under adiabatic conditions. The maps recently from Thome et al. [9] and Cavallini et al. [10] are most quoted. In addition, numerous methods have been proposed to differentiate between stratified and non-stratified condensation, such as those by Dobson and Chato [11]. For a relatively large tube diameter and small heat transfer rate, stratified condensation is studied for the MED system [12]. Cavallini et al. [13], Dobson and Chato [11] concluded that the liquid pool heat transfer at the bottom of the tube should not be negligible at high mass velocity.

Despite the heat transfer performance in a large falling film tube bundle has been studied by previous scholars experimentally or theoretically, discrepancies exist due to the difference in operating conditions or fluids for previous researchers. Besides, the intertube vapor flow on falling film heat transfer coefficient has rarely been taken into account. Comprehensive experiments including three parts each with the study on falling film evaporation, condensation, and intertube vapor flow were conducted obtaining a comprehensive model for the simulation of a large tube bundle using parameter distribution method. The paper aims at discussing the effects of various parameters on flow and heat transfer performance in a large horizontal falling film tube bundle evaporator.

2. Experimental apparatus and methods

Three experiments were carried out each for the study of falling film evaporation outside a single tube, condensation inside a single tube, and vapor flow resistance cross a horizontal falling film tube bundle as shown from Figs. 1–3.

In the experiments, the measuring instrument and sensors are of the same type. Calibration of thermocouples was done before the experiment to control the maximum error within less than 0.1 ℃. The precisions of pressure difference sensor (GE Druck LPX9381) and pressure sensor (UNIK PMP5073) are 1 and 30 Pa, respectively. The estimated uncertainties of all measuring values are less than ±6%.

2.1. Experiment 1: Falling film evaporation outside a single tube

The facility featured a heating tank, a liquid feeder, an evaporator, a condenser, in addition to a liquid feeder and a metering pot as shown in Fig. 1. The test tube is made of HAL77-2A Al-brass with the outer

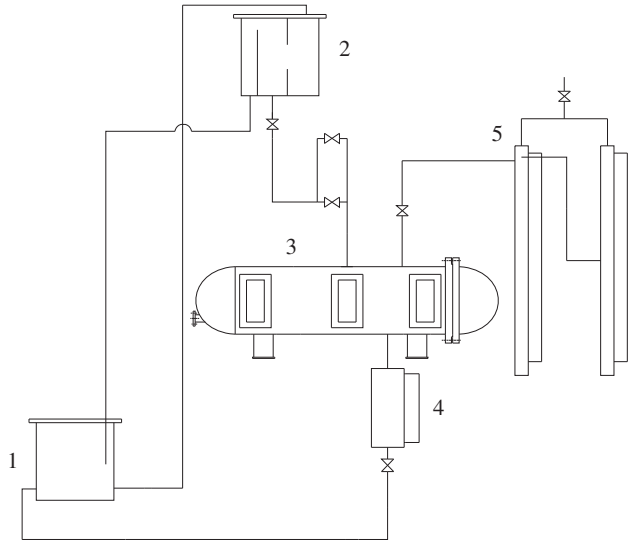

Fig. 1. Schematic sketch of evaporation outside a horizontal tube.

diameter (OD) 25.4 mm, inner diameter (ID) 24 mm, and length 2000 mm. Heat flux is provided by an electric heater embedded inside of the tube and the heat flux is ranging from 0 to 3 kW. To reduce heat losses, the evaporator is covered by thermal insulators, which can guarantee the heat loss of this experiment is less than 7%. The surface of heating tube was grooved in circumference direction with an interval of 45˚ and thermocouples were bedded in the grooves. Thus, the temperatures profile in tube surface could be observed. There is one thermocouple located inside liquid feeder to get liquid temperature. Thereby, the temperature difference between the tube wall temperature and the liquid temperature can be calculated, which is used to calculate the transfer heat coefficient.

In the experiment, water starts from the heating tank where the temperature of the liquid is controlled to the required values, and then it is pumped up to the liquid feeder followed by several regulation valves and a flow meter. From the liquid feeder, the water is supplied at the desired flow rate to the testing cell forming falling films outside horizontal tubes as it continuously flows down. Part of the water evaporates outside the heating tube and turns into vapor. The vapor condenses in the condenser to keep a steady pressure of the cell. The rest of the water is pumped into the heating tank for recycling. During experiments, temperatures are from 50 to 70˚C and liquid flow rates from 0.026 to 0.09 kg/m s.

2.2. Experiment 2: Condensation inside a horizontal tube

As shown in Fig. 2, the test facility consists of a boiler, a test tube divided into five sections, a vapor–liquid separator, two vapor condensers, a condensate tank, and a cooling water tank. The test tube is made of HAL77-2A Al-brass with 25.4 mm OD, 24 mm ID, and 9,000 mm length. For its five sections, every two of the adjacent tubes are connected by a quartz glass tube through which the flow pattern of two phase flow inside could be observed. On each cross-section, thermocouples are set, respectively, for measuring temperatures of the vapor and the condensate, as well as the wall temperatures. Thereby, the temperature difference can be calculated, which is used to calculate the condensation transfer heat coefficient. Both the vapor–liquid separator and the condenser have a liquid meter to measure the condensing rates. Pressure sensors are set at both the inlet and the outlet of test section to measure the steam pressure. The tube side pressure drop of each exchanger is also measured by a differential manometer.

The steam generated from the boiler enters the inside of the test tube where it is cooled by the cooling water outside the tube and condenses along the tube. Surplus steam if any is condensed in the condensers. Stratified flow pattern could be observed after the first section of the testing tube for all operating conditions. During experiments, steam temperature varies from 40 to 70˚C, inlet steam velocity from 20 to 80 m/s, and inlet temperature difference from 4 to 8˚C. This experiment aims at obtaining the condensation heat transfer and pressure drop when steam flows and condenses inside a horizontal tube.

2.3. Experiment 3: Steam flow resistance across tube bundle

As Fig. 3 shows, the experimental setup is mainly comprised of a boiler, a test section, a condenser, and a water tank. Five hundred and one test tubes are made of HAL77-2A Al-brass with 25.4 mm OD, 24 mm ID, and 500 mm length. The tube bundle inside the test section is in the triangular arrangement. The relative tube bundle-pitch ratio is 1.3, a typical value for evaporators used in desalination. Pressure sensors and pressure difference sensors are installed in inlet and outlet of tube bundle to measure pressure drop.

In the experiment, the steam generated from the boiler is supplied to the test section and then passes

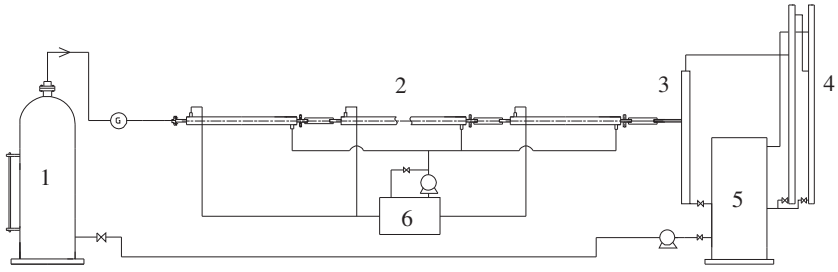

Fig. 2. Schematic sketch of condensation inside a horizontal tube.

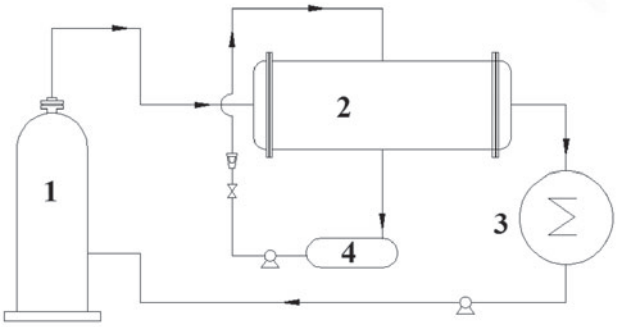

1 Boiler 2 Test section 3 Condenser 4 Water tank

Fig. 3. Schematic sketch of steam flow resistance across tube bundle.

horizontally across the tube bundle along its column direction, while water is flowing downward outside the tubes' surfaces. The temperatures of the liquid and steam are of the same, no heat exchange happens during the two phases. The steam after passing across the tube bundle is condensed at the condenser. Steam velocity calculated by the minimum section area varies between 2 and 12 m/s, liquid flow rate between 0.02 and 0.09 kg/m s and steam temperature between 50 and 70 ℃. Intertube steam pressure drop, across the tube bundle at different liquid flow rate, and temperatures are measured in this experiment.

3. Physical model

Fig. 4(a) shows the configuration of a simplified evaporator. For emphasizing on the heat transfer performance along the tube column direction and length direction, the tube bundle only consists of one row of heating tubes. Within the evaporator, water films outside the tube surfaces while inside the tubes steam flows and condenses along the tube length direction. The vapor generated from the water films horizontally flows across the tube bundle and is condensed in the condenser. Generally, the temperature of steam inside tubes varies along the tube length direction with the heat of steam releasing to the water outside. Besides, due to the accumulation of intertube vapor and its flow resistance, the vapor pressure changes in its flow direction. In this paper, the geometry parameters are described in Table 1.

Table 1
Geometry parameters

Name	Description
Tube material	Alumni-brass
Tube length (m)	8
Column number	78
Tube outside diameter (mm)	25.4
Tube inside diameter (mm)	24
Tube arrangement	Triangular

As interpreted above, for a faster calculation, half the tube bundle column is chosen as the calculation area considering its symmetric configuration in horizontal direction as shown in Fig. 4(a). Likewise, for a better display of the results half of the tube bundle along the tube column direction is shown in each figure with column 1 representing the boundary of the tube bundle while column 39 the center. Fig. 4(b) demonstrates the physical model and grid generation. The subdivision in the j direction is of the same with the tube column numbers, while z denotes each discrete element along the tube length direction. The total grid number is 2,560 with the deviation in calculated heat transfer rate no bigger than 0.02%.

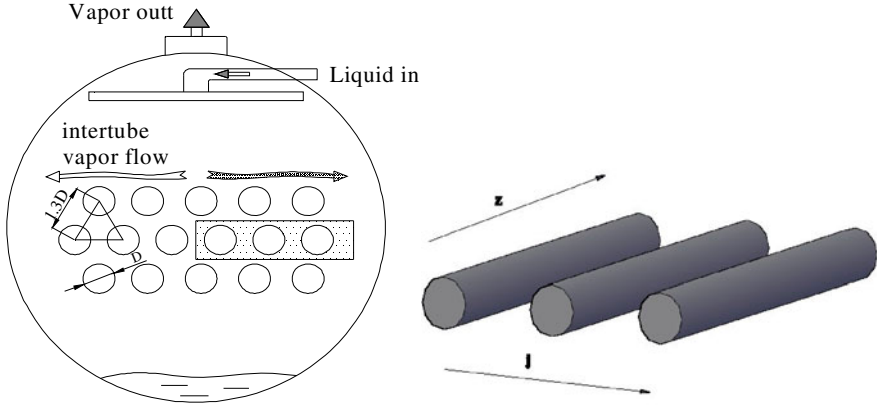

(a) Cross-section of the evaporator (b) Two-dimensional model

Fig. 4. Schematic of falling film evaporator and two-dimensional model.

4. Mathematical model

The calculation of the falling film evaporator is based on the following assumptions:

(1) Uniform distribution of water film is achieved on the tube bundle at the saturated temperature.
(2) Intertube vapor flows in the horizontal direction.
(3) Effects of fouling resistance on heat transfer are neglected.

Three modules are calculated respectively for each unit volume in the calculation area: the water evaporation module, the inside-tube steam module, and the intertube vapor module.

4.1. Outside-tube fresh water evaporation module

Through experiment 1, the heat transfer coefficient of water falling film can be calculated from the related measuring values such as temperature difference ΔT, heat transfer rate q. Furthermore, based on the experimental data the correlation can be proposed as (Eq. (1)):

$$Nu_e = 0.0173\, Re_{\Gamma}^{0.0432} Pr_{\mathrm{e}}^{0.31} \tag{1}$$

where $Re_{\Gamma} = 4\Gamma/\mu$. Under the condition of $190 < Re_{\Gamma} < 890$, $2.69 < Pr_{\mathrm{e}} < 4.13$, Eq. (1) is able to correlate the corresponding sets of data with a standard deviation of ±10%.

4.2. Inside-tube steam module

Through experiment 2, the condensation heat transfer coefficient inside tube is obtained as follows:

$$h_{\mathrm{c}} = (-0.944x^2 + 0.841x + 0.291)\left[\frac{\rho_{\mathrm{l}}(\rho_{\mathrm{l}} - \rho_{\mathrm{st}})g\lambda_{\mathrm{l}}^3 r}{\mu_{\mathrm{l}} D_{\mathrm{c}} \Delta T_{\mathrm{c}}}\right]^{0.25} \tag{2}$$

The steam pressure drop is also experimentally measured in experiment 2 and a valid equation was correlated as follows:

$$Eu_{\mathrm{c}} = 11.2 Re_{\mathrm{st}}^{-0.234} x^{3/5},\ Eu_{\mathrm{c}} = \frac{\Delta P_{\mathrm{c}}}{\rho_{\mathrm{st}} u_{\mathrm{st}}^2} \tag{3}$$

where $Re_{\mathrm{e}} = \frac{u_{\mathrm{st}} \cdot D_{\mathrm{st}}}{\nu}$, $Re_{\Gamma} = 4\Gamma/\mu$.

Eqs. (2) and (3) are fitted in the scope of $Re_{\mathrm{st}} < 30{,}000$, $0 < \chi < 1$, which correlate the corresponding sets of data with a standard deviation of ±15%.

The calculation is along the tube length direction:

$$P_{\mathrm{c,j,z}} = P_{\mathrm{c,j,z-1}} - \Delta P_{\mathrm{c,j,z-1}} \tag{4}$$

The boundary conditions are:

$$T_{\mathrm{c,j,z}} = T_{\mathrm{c,initial}},\ \text{for } j = 1, 2, \ldots, N_{\mathrm{j}},\ \text{at } z = 1 \tag{5}$$

$$\Delta P_{\mathrm{c,j,z}} = \Delta P_{\mathrm{c,initial}},\ \text{for } j = 1, 2, \ldots, N_{\mathrm{j}} \tag{6}$$

where $T_{\mathrm{c,initial}}$ is the inlet steam temperature of tube bundle and $\Delta P_{\mathrm{c,initial}}$ represents the total pressure drop between inlet and outlet of the first column tube.

4.3. Intertube vapor module

Through experiment 3, the intertube vapor pressure drops were experimentally measured and correlated as (Eq. (7)):

$$Eu_{\mathrm{e}} = 23.1 Re_{\mathrm{e}}^{-1.1} Re_{\Gamma}^{0.926} + 4.07 Re_{\mathrm{e}}^{-0.216},\ Eu_{\mathrm{e}} = \frac{2}{N}\frac{\Delta P_{\mathrm{e}}}{\rho_{\mathrm{e}} u_{\mathrm{e}}^2} \tag{7}$$

where $Re_{\mathrm{e}} = \frac{u_{\mathrm{e}} \cdot D_{\mathrm{e}}}{\nu}$, $Re_{\Gamma} = 4\Gamma/\mu$. Under the experimental conditions of Re_{e} within 600–3,300, Re_{Γ} within 140–680, Eq. (7) is able to correlate the corresponding sets of data with a standard deviation of ±10%.

The calculation is along the tube column direction:

$$P_{\mathrm{e,j,z}} = P_{\mathrm{e,j-1,z}} + \Delta P_{\mathrm{e,j-1,z}} \tag{8}$$

The boundary conditions are as follow:

$$P_{\mathrm{e,j,z}} = P_{\mathrm{e,initial}},\quad \text{for } z = 1, 2, \ldots,\ \text{at } j = 1 \tag{9}$$

4.4. Governing equations

For every unit volume, the heat transfer rate for evaporation side equals to that on the condensation side:

$$h_{\mathrm{e}} A_{\mathrm{e}} \Delta T_{\mathrm{e}} = h_{\mathrm{c}} A_{\mathrm{c}} \Delta T_{\mathrm{c}} \tag{10}$$

For the start of every unit volume, the overall temperature difference ΔT is a known value.

5. Algorithm

The algorithm of the model is introduced in Fig. 5. To be mentioned, the total steam pressure drop of the first tube $\Delta P_{\mathrm{c,initial,1,1}}$ is calculated at the very beginning as $\Delta P_{\mathrm{c,initial}}$ and it serves as a boundary condition for the calculation of the rest of tube bundle as illustrated in Eq. (6). For every unit volume, the values of three modules are updated each iteration. The initial

hypothetical values are modified until the convergence of all parameters is reached.

6. Result and discussion

6.1. The heat transfer coefficient distribution

Fig. 6(a) and (b) demonstrate the variation of overall heat transfer coefficient h at different working conditions. It is noted that the heat transfer performance increases with the tube length, reaches a maximum, and then declines with the steam further flowing along the inside of the tube. The lowering value of h near the entrance is mostly likely due to a certain degree of superheat of steam caused by the steam flow resistance before the entrance. The single phase heat exchange of steam inside the tube leads to the lower overall heat transfer coefficient near the entrance. Besides, the high steam velocity near the entrance might have an unfavorable effect on the formation of a stable condensation film through the observation of experiment and thus might consequently lead to a lower value of h near the entrance. As steam flows and condenses inside of the tube, the superheat is gradually eliminated and the condensation heat transfer gradually dominates the heat transfer process, h shows an increasing trend. As steam

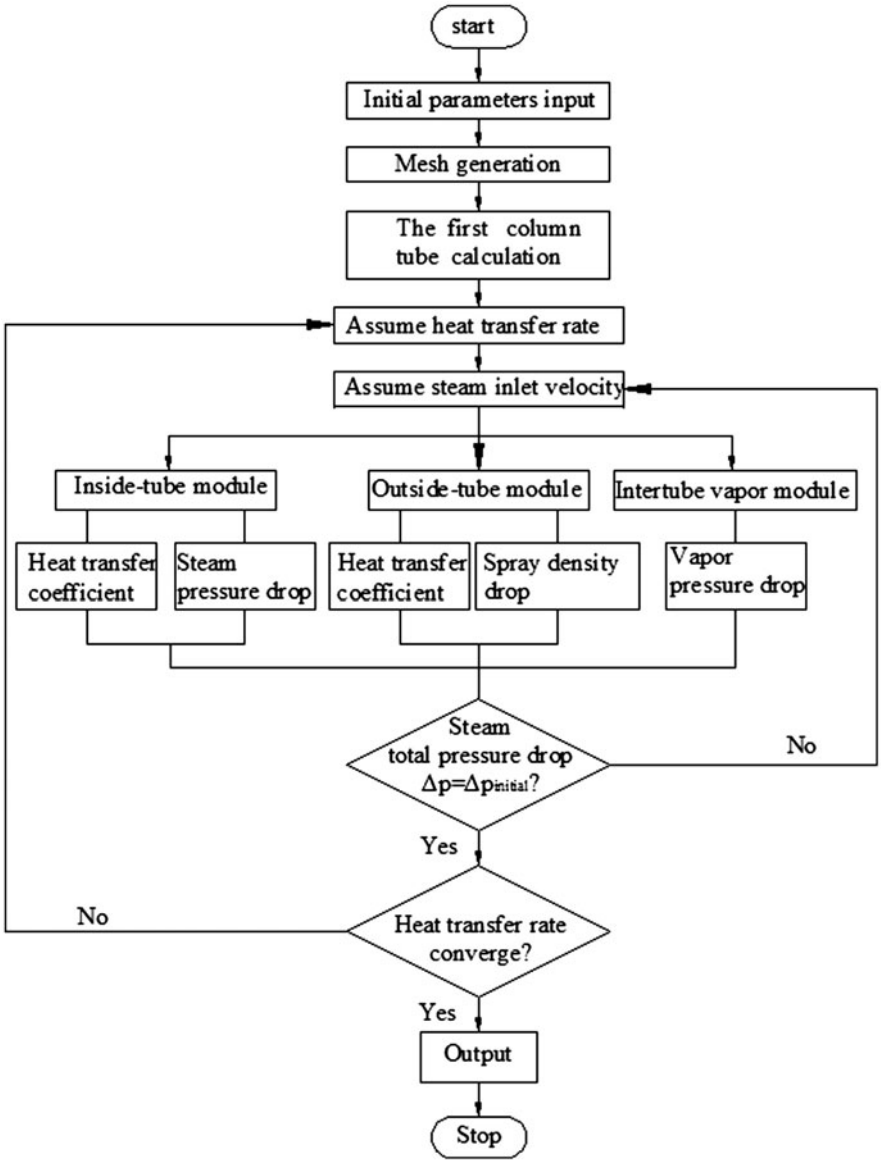

Fig. 5. Flowchart of the numerical algorithm.

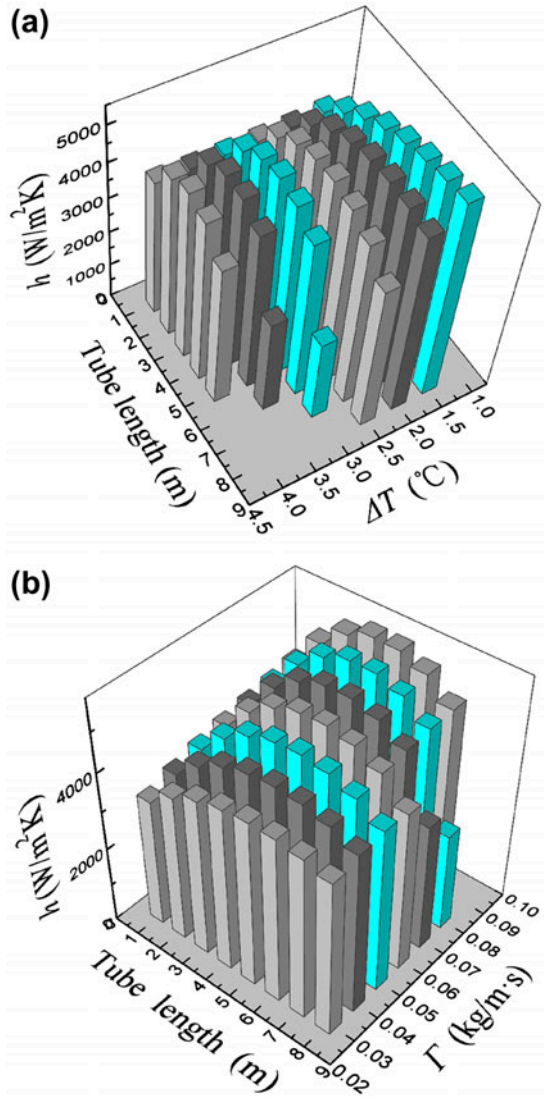

Fig. 6. Heat transfer coefficient distribution.

further flows and condenses along the tube length, h gradually decreases. It is associated with the continuous accumulation of condensate at the bottom of the tube. As the decrease of steam velocity together with the accumulation of condensate along the tube length, the shear force of the steam on the condensate becomes weaker which leads to the rise of the liquid level at the bottom. More area of heat transfer surface is then covered by the liquid, while the liquid single phase heat transfer coefficient at the bottom is much smaller compared with the steam condensation heat transfer coefficient. Heat transfer coefficient h then decreases along after a maximum value.

With the increase of temperature difference ΔT, seen in Fig. 6(a), h exhibits a decreasing trend. This also has close relation with the condensation heat transfer process inside the tubes. As the heat transfer rate increases with ΔT, the liquid film both near the wall surface becomes thicker which weakens the condensation heat transfer performance. Besides, in Fig. 6(a), it is apparent that with the increase of ΔT, the required tube length is reduced for the complete condensation of a constant amount of steam. Fig. 6(b) shows that h increases with the increase of water spray density Γ. This is mainly due to the increase of turbulence in the liquid film which enhances the evaporation heat transfer performance. It is noticed that at the end of the tube length, with the increment of Γ, h shows a decreasing trend. It is because as Γ increases, more condensate accumulates at the bottom end of the tube which deteriorates the heat condensation transfer performance and leads to a lower value of h.

6.2. The temperature and vapor velocity distributions

The flow of vapor across the tube bundle generates flow resistance among the tubes; thus, the saturation evaporation temperature varies along the tube column direction. While flowing from the center of the tube bundle to the boundary, the vapor continuously accumulates resulting different flow resistance along the flow direction.

Fig. 7 shows the variation of vapor velocity among the tubes. Along the tube column direction, as the intertube vapor flows from the center (column number is 39) to the boundary (column number is 1), its velocity gradually increases. Along the tube length direction, it has a maximum value within its effective heat transfer length. The velocity distribution has a similar trend with h along this direction due to the increase in heat transfer rate, firstly, and decrease in heat transfer rate after a maximum value is attained. Fig. 8 demonstrates that the vapor temperature T_e

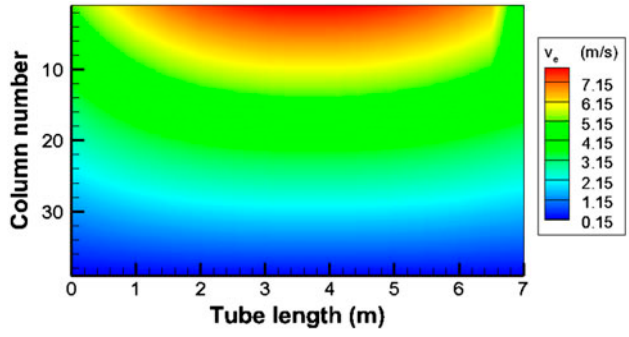

Fig. 7. Vapor velocity distribution.

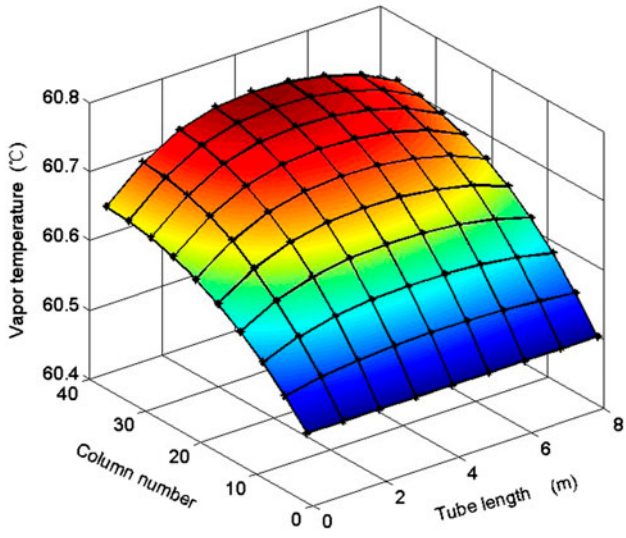

Fig. 8. Vapor temperature distribution.

exhibits an exponential increasing trend with the increase in the tube column number. As the vapor flows from the center to the boundary of the bundle, the closer the vapor is to the boundary, the bigger is the change in the vapor temperature.

6.3. The distributions of local vapor temperature drop dT

As discussed above, the vapor temperature T_e varies among the tubes. Here, we define dT as the temperature difference between the local vapor temperature and the bulk vapor temperature of the evaporator. Fig. 9 demonstrates the variation of dT along the tube column direction at different working conditions. In Fig. 9(a)–(c), it is noted that dT increases with the column number. Fig. 9(a) and (b) show that along the tube column direction, dT has a larger gradient near the boundary when ΔT or Γ has a larger value. It is related to the local vapor speed, the higher the local vapor speed, the larger the temperature drop. With the increase of ΔT, more vapors are generated that lead to a higher speed of vapor among tubes, thus dT is increasing gradually as seen in Fig. 9(a). When Γ is increased, the liquid films outside the tubes become thicker and the flow area for the intertube vapor becomes smaller that result in larger vapor speed and consequent larger temperature drop as shown in Fig. 9(b). Evaporation temperatures also affect dT. With the evaporation temperature increases, the vapor specific volume becomes smaller which results in lower vapor speed and smaller dT, see Fig. 9(c).

Due to the vapor temperature variance among the tubes along the tube column direction, the heat transfer rate q also shows an uneven distribution as

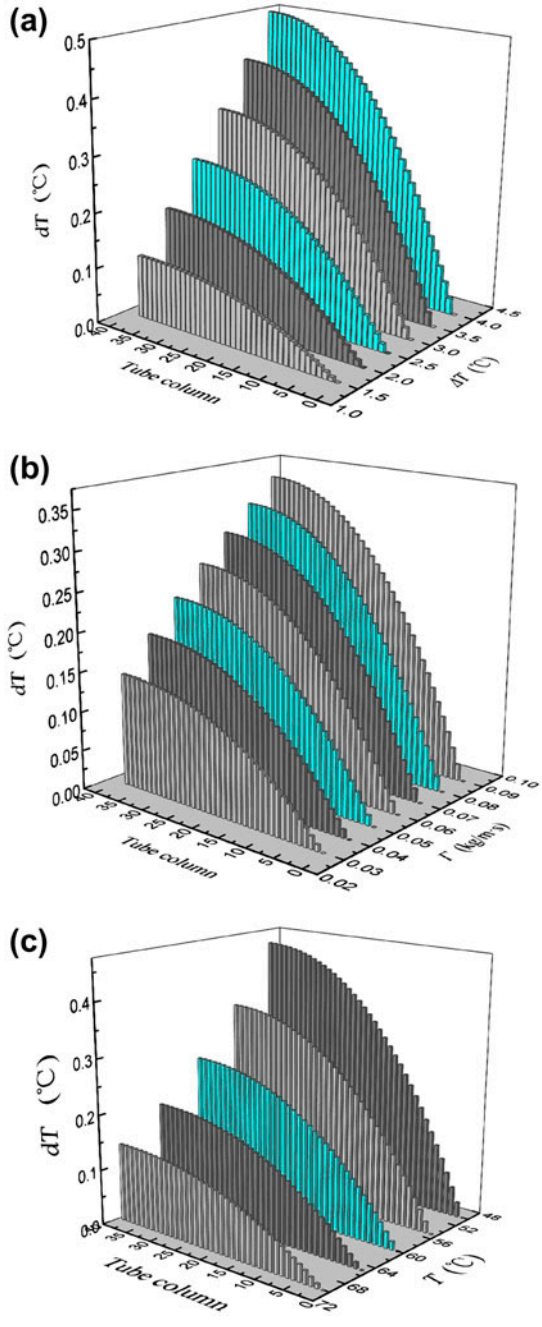

Fig. 9. Temperature drop distributions.

demonstrated in Fig. 10. As the vapor temperature increases with the tube column number, the overall temperature difference decreases along this direction, so q also decreases with the tube column number. Moreover, because every tube has the same fore and aft steam pressure difference, due to the variance in the q along the tube length direction, the inlet steam velocity u_{in} also changes in this direction to keep the pressure balance.

6.4. The bundle effect on the utilization of initial temperature difference

Fig. 11 demonstrates the bundle effect on the distribution of evaporation temperature with the change of the design of the total column number (CN). It is indicated that the larger CN the bundle includes, the more rapidly the rising of the vapor temperature from the boundary to the center. As steam flows from the center to the boundary, the larger value of CN, the more the vapor accumulates at the same column number which results in a higher vapor temperature.

The vapor temperature drop dT within the tube bundle directly results in the reduction in the overall temperature difference, which weakens the heat transfer. For analyzing the affect of dT on ΔT, the parameter Φ is defined featuring the ratio of the maximum temperature drop dT_{max} to the temperature difference at inlet ΔT:

$$\Phi = \frac{dT_{max}}{\Delta T} \times 100\% \quad (11)$$

Fig. 12 shows the Φ increases with the increment of ΔT. Take CN = 70 as an example, when $\Delta T = 1.5$℃, Φ is 22.6%, when $\Delta T = 4$℃, Φ is 34.4%. It also indicates that the more the CN, the larger value of Φ, as shown in Fig. 12. The parameter Φ can evaluate the heat transfer performance to a certain extent. The greater the value of Φ means that dT reduces larger the proportion of ΔT, which weakens the heat transfer.

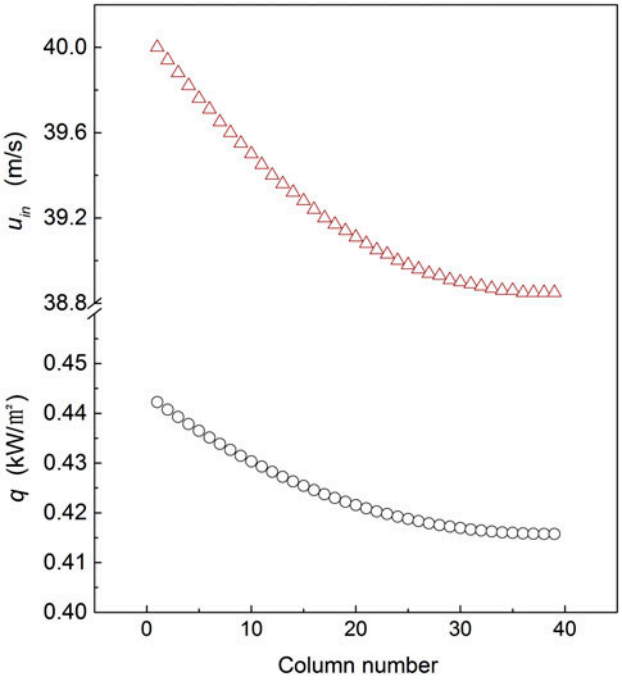

Fig. 10. The steam inlet velocity and heat transfer rate distributions along the tube column direction.

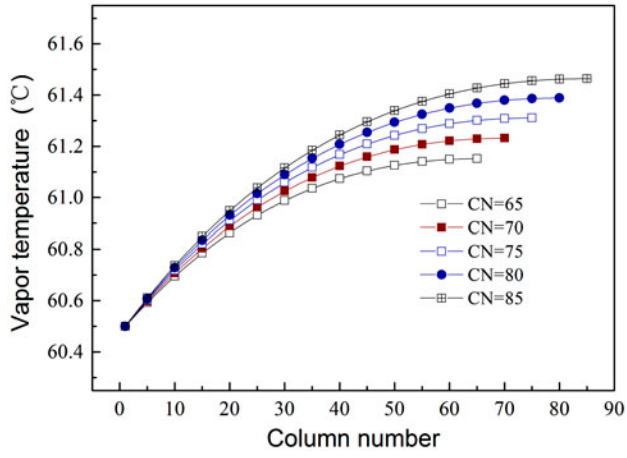

Fig. 11. The vapor temperature distribution with the change of total column number of the bundle.

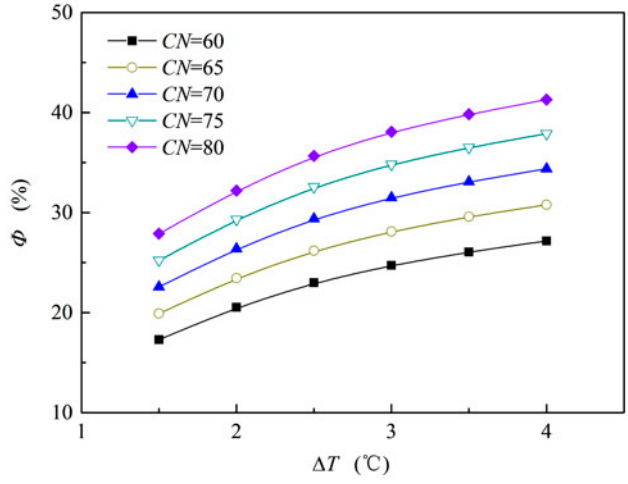

Fig. 12. The variance of Φ with the change of tube column number and temperature difference.

7. Concluding remarks

A comprehensive model has been developed based on a series of experiments to study the effects of the operating conditions on the heat transfer performance, as well as parameters' distributions in a falling film horizontal tube bundle evaporator. The results suggest the following conclusions:

(1) The variation of overall heat transfer coefficient h along the tube length direction is mainly determined by the condensation heat

transfer performance inside the tubes which shows an increasing trend firstly and decreasing after reaching a maximum value.

(2) The flow and accumulation of vapor among tubes causes vapor resistance and lead to temperature drop dT along the flow direction. The dT increases with the increment of water flow rate, the temperature difference, and the evaporation temperature.

(3) Due to the change of vapor temperature, the heat transfer rate and steam inlet velocity decreases along the tube column direction.

(4) The more column numbers the tube bundle includes, the dT will reduce larger proportion of temperature difference ΔT, which weakens the heat transfer.

Acknowledgments

This work is supported by the key project of Chinese National Natural Science Foundation (No. 51336001). The authors are grateful for its financial support.

Nomenclature

A — heat transfer area, m^2
CN — the column number that the tube bundle includes
D — diameter of tube, m
dT — temperature drop along the tube length, ℃
g — gravitational acceleration, m/s^2
h — local heat transfer coefficient, $W/m^2{\cdot}K$
N — tube column number that the intertube vapor has passed across
N_z — grid number along tube length
Nu — nusselt number
Pr — prandtl number
P — pressure, Pa
ΔP — pressure drop, Pa
q — heat transfer rate, kW/m^2
Re — reynolds number
Re_Γ — falling film Reynolds number
T — temperature, ℃
ΔT — temperature difference at inlet, ℃
u — velocity, m/s
x — vapor local quality
j, z — space coordinates

Greek symbols

Γ — liquid flow rate, kg/m s
λ — thermal conductivity, W/m K
μ — dynamic viscosity, N s/m^2
ρ — density, kg/m^3
υ — kinematic viscosity, m^2/s
Φ — ratio of the max temperature drop to the temperature difference at inlet

Subscripts

c — condensation side
e — vapor on the evaporation side
initial — parameters' initial values
in — inlet of each tube
l — liquid on the condensation side of the inner tube
local — parameters' local value
max — the maximum value
st — steam on condensation side of the inner tube

References

[1] Y. Fujita, M. Tsutsui, Experimental investigation of falling film evaporation on horizontal tubes. Heat Transfer—Jpn. Res. 27 (1998) 609–618.
[2] Z.H. Liu, Q.Z. Zhu, Y.M. Chen, Evaporation heat transfer of falling water film on a horizontal tube bundle, Heat Transfer—Asian Res. 31 (2002) 42–55.
[3] W.H. Parken, L.S. Fletcher, V. Sernas, J.C. Han, Heat transfer through falling film evaporation and boiling on horizontal tubes, J. Heat Transfer 112 (1990) 744–750.
[4] G. Ribatski, J.R. Thome, Experimental study on the onset of local dryout in an evaporating falling film on horizontal plain tubes, Exp. Therm. Fluid Sci. 31 (2007) 483–493.
[5] S.Q. Shen, G.T. Liang, L.Y. Gong, X.S. Mu, R. Liu, X.H. Liu, Space distribution of heat transfer performance in horizontal tube falling film evaporator, CIESC J. 62 (2011) 3381–3385 (in Chinese).
[6] X. Zeng, M.C. Chyu, Z.H. Ayub, Experimental investigation on ammonia spray evaporator with triangular-pitch plain-tube bundle, Part II: Evaporator performance, Int. J. Heat Mass Transfer 44 (2001) 2081–2092.
[7] L. Xu, M. Ge, S. Wang, Y. Wang, Heat-transfer film coefficients of falling film horizontal tube evaporators, Desalination 166 (2004) 223–230.
[8] X. Zeng, M.C. Chyu, Z.H. Ayub, Experimental investigation on ammonia spray evaporator with triangular-pitch plain-tube bundle, Part I: Tube bundle effect, Int. J. Heat Mass Transfer 44 (2001) 2299–2310.
[9] J. El Hajal, J.R. Thome, A. Cavallini, Condensation in horizontal tubes, Part 1: Two-phase flow pattern map, Int. J. Heat Mass Transfer 46 (2003) 3349–3363.
[10] A. Cavallini, G. Censi, D.D. Col, G.A. Doretti, L. Rossetto, In-tube condensation of halogenated refrigerants, ASHRAE Trans. 108 (2002) 146–161.
[11] M.K. Dobson, J.C. Chato, Condensation in smooth horizontal tubes, J. Heat Transfer 120 (1998) 193–213.
[12] S. Shen, R. Liu, Y. Yang, X. Liu, J. Chen, Condensation character of a stratified flow inside a horizontal tube, Desalin. Water Treat. 33 (2011) 218–223.
[13] A. Cavallini, G. Censi, D. Del Col, L. Doretti, G.A. Longo, L. Rossetto, C. Zilio, Condensation inside and outside smooth and enhanced tubes—A review of recent research, Int. J. Refrig. 26 (2003) 373–392.